nature geoscience

REVIEW ARTICLE

PUBLISHED ONLINE: 28 NOVEMBER 2013 | DOI: 10.1038/NGEO2009

Projected response of the Indian Ocean Dipole to greenhouse warming

Wenju Cai[1,2]*, Xiao-Tong Zheng[2,3], Evan Weller[1], Mat Collins[4], Tim Cowan[1], Matthieu Lengaigne[5], Weidong Yu[6] and Toshio Yamagata[7]

Natural modes of variability centred in the tropics, such as the El Niño/Southern Oscillation and the Indian Ocean Dipole, are a significant source of interannual climate variability across the globe. Future climate warming could alter these modes of variability. For example, with the warming projected for the end of the twenty-first century, the mean climate of the tropical Indian Ocean is expected to change considerably. These changes have the potential to affect the Indian Ocean Dipole, currently characterized by an alternation of anomalous cooling in the eastern tropical Indian Ocean and warming in the west in a positive dipole event, and the reverse pattern for negative events. The amplitude of positive events is generally greater than that of negative events. Mean climate warming in austral spring is expected to lead to stronger easterly winds just south of the Equator, faster warming of sea surface temperatures in the western Indian Ocean compared with the eastern basin, and a shoaling equatorial thermocline. The mean climate conditions that result from these changes more closely resemble a positive dipole state. However, defined relative to the mean state at any given time, the overall frequency of events is not projected to change — but we expect a reduction in the difference in amplitude between positive and negative dipole events.

Anthropogenic emissions of carbon dioxide have induced widespread warming of the world oceans[1,2]. Over the past few decades, surface warming in the tropical Indian Ocean has not been spatially uniform. In austral spring, the eastern tropical Indian Ocean warms slower than the west[3]. The associated trend in zonal sea surface temperature (SST) gradient is consistent with a long-term change in the Indian Ocean Dipole (IOD), the dominant mode of year-to-year variability of the tropical Indian Ocean. The IOD usually peaks in the spring season, and its positive phase (pIOD) is characterized by SSTs lower than normal in the eastern tropical Indian Ocean but warmer in the west[4–7], and vice versa for a negative IOD (nIOD) phase. Commonly measured by a dipole mode index (DMI) — defined as the difference of SST anomalies in the west (50° E to 70° E and 10° S to 10° N) minus east (90° E to 110° E and 10° S to 0°) equatorial Indian Ocean[4] — the index has displayed an upward trend since the 1950s[8], congruent with the slower warming rate of the eastern tropical Indian Ocean embedded in the spring warming pattern[3].

The upward trend of the DMI translates into an increased frequency of pIOD events in recent decades[8–10], including the occurrence of three consecutive pIOD events during 2006–2008. These have devastating impacts, including droughts in East Asia[11] and Australia[8,12–14], and flooding in parts of the Indian subcontinent[15] and East Africa[16,17], as well as altering the relationship between the El Niño/Southern Oscillation (ENSO) and the Asian monsoon[18]. Such events also precondition major wildfires in southeast Australia[19], initiate coral reef death across western Sumatra[20] and exacerbate malaria outbreaks in east Africa[21]. These severe impacts raise the question as to whether the increased frequency of pIOD events is a manifestation of a gradual anthropogenic climate change signal.

The main mode of variability in the tropical Pacific Ocean is ENSO, and at first glance this well-studied phenomenon may seem to be analogous to the IOD. However, the tropical Indian Ocean differs from the tropical Pacific in several climatically important ways. Chief among these is its close proximity to the Asian continent and the associated strong seasonal Asian monsoon[22–24]. As a result, the equatorial Indian Ocean lacks steady easterly winds. The long-term mean winds along the equatorial Indian Ocean are westerlies, but these equatorial westerlies are weakest from June to November, when east-to-southeasterly winds prevail off the Sumatra–Java coast, lifting the thermocline (the dynamic depth of the largest vertical temperature gradient in the upper ocean). When the anomalous easterlies are strong enough, the thermocline is lifted to a depth shallow enough to influence SST, facilitating the development of a pIOD event[4–7].

The IOD often interacts and frequently occurs with, or just before, ENSO events[25–28], and can also be triggered by variability within the Asian summer monsoon[23,24]. However, its dynamic source lies within the Indian Ocean[4,5]. Specifically, anomalous zonal SST gradients within the tropical Indian Ocean are accompanied by coherent variations in the structure of the subsurface ocean, a strengthening and weakening of the equatorial winds, and spatial shifts in the position of atmospheric convection and global teleconnections that drive changes in rainfall and weather patterns in many parts of the world[10,29,30].

Many feedbacks that operate in the Indian Ocean associated with the IOD are analogous to what occurs in the tropical Pacific. These include a positive feedback loop, referred to as the Bjerknes feedback[31], involving zonal SST gradients that drive zonal wind anomalies, which in turn lead to a changing thermocline[32–36], with the effect of reinforcing the SST gradients.

[1]CSIRO Marine and Atmospheric Research, Aspendale, Victoria, Australia, [2]Physical Oceanography Laboratory, Qingdao Collaborative Innovation Center of Marine Science and Technology, Ocean University of China, Qingdao, China, [3]Key Laboratory of Ocean–Atmosphere Interaction and Climate in Universities of Shangdong, Ocean University of China, Qingdao, China, [4]College of Engineering Mathematics and Physical Sciences, Harrison Building, Streatham Campus, University of Exeter, Exeter, UK, [5]Laboratoire d'Océanographie et du Climat: Expérimentation et Approaches Numériques (LOCEAN), IRD/UPMC/CNRS/MNHN, Paris, France, [6]First Institute of Oceanology, State Ocean Administration, Qingdao, China, [7]Application Laboratory, JAMSTEC, 3173-25 Showa-machi, Kanazawa-ku, Yokohama 236-0001, Japan. *e-mail: Wenju.Cai@csiro.au

Box 1 | Characteristics and processes associated with a pIOD

Seasonal phase locking. A pIOD typically develops and matures in the months from June to November. In association with the onset, transition and decay of the Asian monsoon, easterlies over the Sumatra-Java latitudes are present only during these months, when the thermocline is lifted to a shallow enough depth to be able to influence SSTs. In December, a pIOD terminates abruptly as the winds change to westerlies, marking the onset of the Australian summer monsoon.

Indo-Pacific Walker circulation. This is the zonally oriented component of the atmospheric circulation. Under normal conditions, surface westerlies over the far northeastern equatorial Indian Ocean and equatorial easterly trade winds in the Pacific flow towards convective towers over the west Pacific and the maritime continent. In the Pacific, the rising air flows eastwards, descending in the east Pacific, and then flows westwards at the surface as the equatorial trade winds. In the eastern tropical Indian Ocean, the rising air flows westwards; however, the descending branch is not as well defined, as indicated by a grey arrow in Fig. 2.

Bjerknes feedback. A positive feedback loop, similar to that which operates in the equatorial Pacific, amplifies incipient pIOD events. An increase in easterly winds off Sumatra-Java induces a shoaling thermocline, enhanced westward-flowing currents and strengthened upwelling. This leads to an anomalous west-minus-east SST gradient. The SST gradient in turn leads to a shift in atmospheric convection towards the west, enhancing the easterly winds off the Sumatra-Java coast. This shift can also reverse the equatorial winds to easterlies. In addition to the response of the thermocline to winds, the Bjerknes feedback also involves the response of SST to variations in the thermocline, and the response of zonal winds to zonal SST gradients, further discussed below.

Thermocline–SST feedback. Stronger-than-normal easterlies over Sumatra-Java or along the equatorial Indian Ocean during June-November lift the thermocline off the Sumatra-Java coast to a depth whereby upwelling cools the SST. The cooling off Sumatra-Java contributes to an anomalous west-minus-east SST gradient, further enhancing the easterlies. The surface and subsurface temperature coupling is a key process of the Bjerknes feedback for a pIOD event and its evolution.

Feedback between zonal wind and zonal SST gradient. An anomalous west-minus-east SST gradient leads to stronger easterlies over the equatorial Indian Ocean and off Sumatra-Java, strengthening the thermocline–SST feedback, and further enhancing the zonal SST gradient. The response of surface zonal winds is linked to convection and precipitation changes induced by SST variations. As such, this is also referred to as part of the associated atmospheric processes.

SST–cloud–radiation feedback. Variability of SST over the eastern tropical Indian Ocean induces variations in clouds, precipitation, convection and fluxes of heat between the atmosphere and the ocean. A surface cooling off Sumatra–Java suppresses convection, cloud cover and precipitation, leading to increased shortwave radiation into the ocean. This in turn dampens the cooling, resulting in a negative feedback mechanism.

Wind–evaporation–SST feedback. SST variability over the eastern tropical Indian Ocean induces variations in winds, wind speed and evaporative heat loss from the ocean to the atmosphere. During the development phase of a pIOD, when SST anomalies are small, an easterly wind anomaly over Sumatra–Java superimposes on the climatological easterlies. The increased wind speed enhances the ocean-to-atmosphere heat loss. Such conditions are conducive to enhanced cooling off the Sumatra–Java coast and pIOD formation. However, the nature of this feedback changes with the seasons: when superimposed on climatological westerly winds due to the onset of the Australia monsoon (typically early December), an easterly wind anomaly leads to a reduction in evaporative heat loss, giving rise to a warming tendency and facilitating the demise of a pIOD event.

IOD skewness. The amplitude of pIOD events tends to be greater than that of nIOD events; this asymmetry is referred to as the IOD positive amplitude skewness. Cool SST anomalies off Sumatra–Java during pIOD events grow larger than warm anomalies during nIOD events. This is because the mean thermocline in the eastern Indian Ocean is deep, and as such a shoaling thermocline induces a cooling through the thermocline–SST feedback during pIOD events. However, this feedback is weaker during nIOD events when the thermocline deepens from the already deep mean position. The amplitude asymmetry means that IOD feedback processes and resultant impacts are stronger during pIOD events, as the signals are better able to manifest out of stochastic noise.

Despite the late realization of its importance, research over the past 15 years has enabled a good understanding of the fundamental dynamic and thermodynamic processes involved in the IOD and its associated nonlinear features[37–44] (see Box 1). An IOD-like variability pattern is found to be simulated in the majority of coupled general circulation models (CGCMs)[45–57]. These CGCMs provide a useful tool for examining the physical processes and feedbacks underlying the IOD and their responses to greenhouse warming.

Here we review the current state of understanding as to how the austral spring mean climate of the tropical Indian Ocean, the IOD and its nonlinear features may be affected by global climate change. We focus on the changes in the physical climate system that have occurred in recent decades, and examine what might happen in the twenty-first century under increasing greenhouse gas emissions.

The IOD in the observed and simulated climate

We reconstructed the austral spring DMI for the twentieth century using a selection of data products[58–60]. The index from two of the products[58,59] displays a clear upward trend in recent decades, whereas the DMI from the third[60] is flat, highlighting the associated uncertainty in the reconstructions. Using the 1961–1990 mean climate as a reference[61], we define an IOD event as when the DMI (ref. 4) crosses a threshold value of 0.75 of the standard deviation (dashed line, Fig. 1a), and calculate pIOD events over 31-year sliding periods. The frequency has increased to an unprecedented level of 12 pIOD events in the past 31 years (solid curve, Fig. 1b), consistent with the increasing frequency seen in other studies[9]. Using a reference to a fixed-period mean climate to identify pIOD events has become widely adopted, and reflects the way in which pIOD occurrences and their impacts are forecast and experienced. Indeed, this behaviour is simulated in CGCM experiments of the twentieth century climate and beyond under projected emission scenarios (Fig. 1c,d), and is in agreement with results in a set of perturbed physics ensemble (PPE) experiments (Fig. 1e,f)[62].

However, if the variance on timescales longer than nine years, including decadal and greenhouse-induced trends, is removed

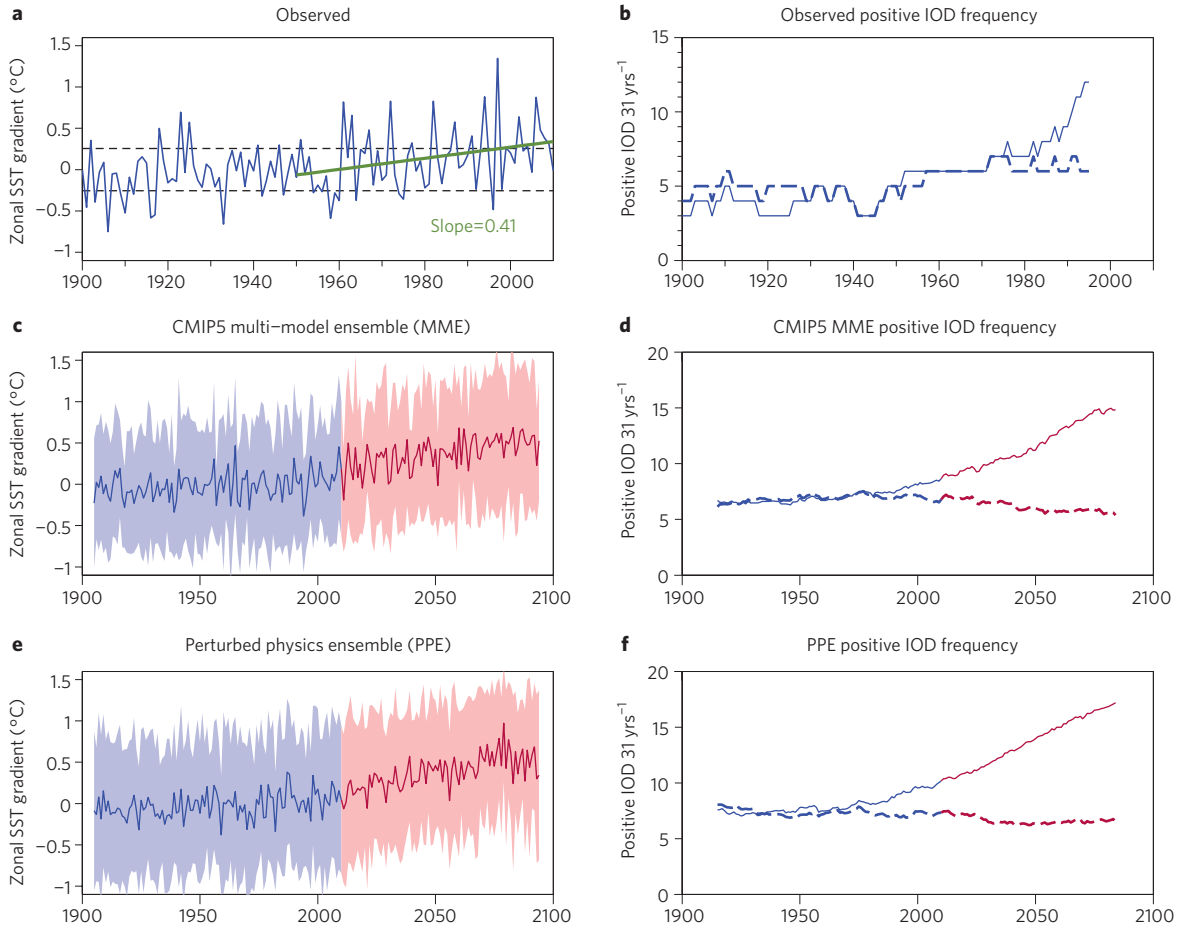

Figure 1 | Observed and projected changes in IOD variability. a, The observed dipole mode index (DMI, °C)[4]. Dashed horizontal lines indicate the 0.75 standard deviation threshold, and the green line indicates the linear trend since 1950. **b**, Number of observed positive IOD events (defined as when the DMI is greater than the 0.75 standard deviation) in 31-year sliding periods (recorded at the 16th year) with (solid) and without (dashed) the long-term climate change signal. **c**, The multi-model ensemble mean DMI (°C) of the historical period (blue) and beyond (red) under projected emission scenarios (Representative Concentration Pathway (RCP)8.5) from the Coupled Model Intercomparison Project phase 5 (ref. 57); the one standard deviation among models is shaded. **d**, Same as **b**, but based on the time series discussed in **c**. **e**,**f**, Same as **c** and **d**, respectively, but from a perturbed physics ensemble with the HadCM3 model[62].

from the time series, a similar count does not indicate a substantial change in the pIOD occurrences, either in observations (blue dashed curve, Fig. 1b) or in the CGCM experiments (blue dashed curves, Fig. 1d,f). Therefore the increasing occurrences in the presence of climate-change-induced trends are generated because of a gradual increase in the mean west-minus-east SST gradient in the tropical Indian Ocean. The gradual increase causes the DMI to cross the defined pIOD threshold more frequently at the end of the twentieth century. Such an enhanced west-minus-east SST gradient is projected to continue into the twenty-first century (Fig. 1c,e). Thus, to assess and understand possible changes in the IOD, it is a common practice to separate out the reference time-evolving mean climate from the anomalies above and below it.

Mean climate changes

The enhanced west-minus-east SST gradient in the future mean climate is produced across different CGCMs (refs 55,63). This is consistent with a projected long-term weakened Walker circulation of the Indo-Pacific[63–66], which is the zonally oriented component of the tropical Indian and Pacific atmospheric circulation. Under normal conditions, air rises in convective towers in the western Pacific and eastern Indian oceans slightly north of the Equator, flows westwards, descends in the western Indian Ocean, and then flows eastwards at the surface. This Walker circulation is projected to weaken, consistent with an observed weakening since 1950[67]. However, the observed Walker circulation stabilized in the 1970s and began to strengthen from the late 1990s[68,69], so much so that the strengthening trend remains when data since the 1970s[70] are included. Although this recent intensification casts doubt on the projected long-term weakening[71], it is not clear to what extent the observed short-term strengthening is driven by climate change or multi-decadal variability.

In a multi-model ensemble average, the variability-induced component is largely removed because each model produces its own variability, which is independent from one model to another. The projected long-term weakening in the Walker circulation arises from a response in the global hydrological cycle. As the global mean saturated water vapour pressure rises with the global mean temperature (at approximately 7% per degree K of warming, according to the Clausius–Clapeyron relationship[66]), the relative humidity remains largely constant such that the global mean vapour pressure also rises at approximately the same rate. The global mean precipitation rate, however, rises at a much smaller rate of around 2% per degree K (ref. 65). The disparity renders a reduction in the rate of exchange of moist boundary layer air with the drier air above, and in vertical motion in the main convective regions of the tropics, leading to a general reduction in the strength of the atmospheric vertical overturning circulation[64].

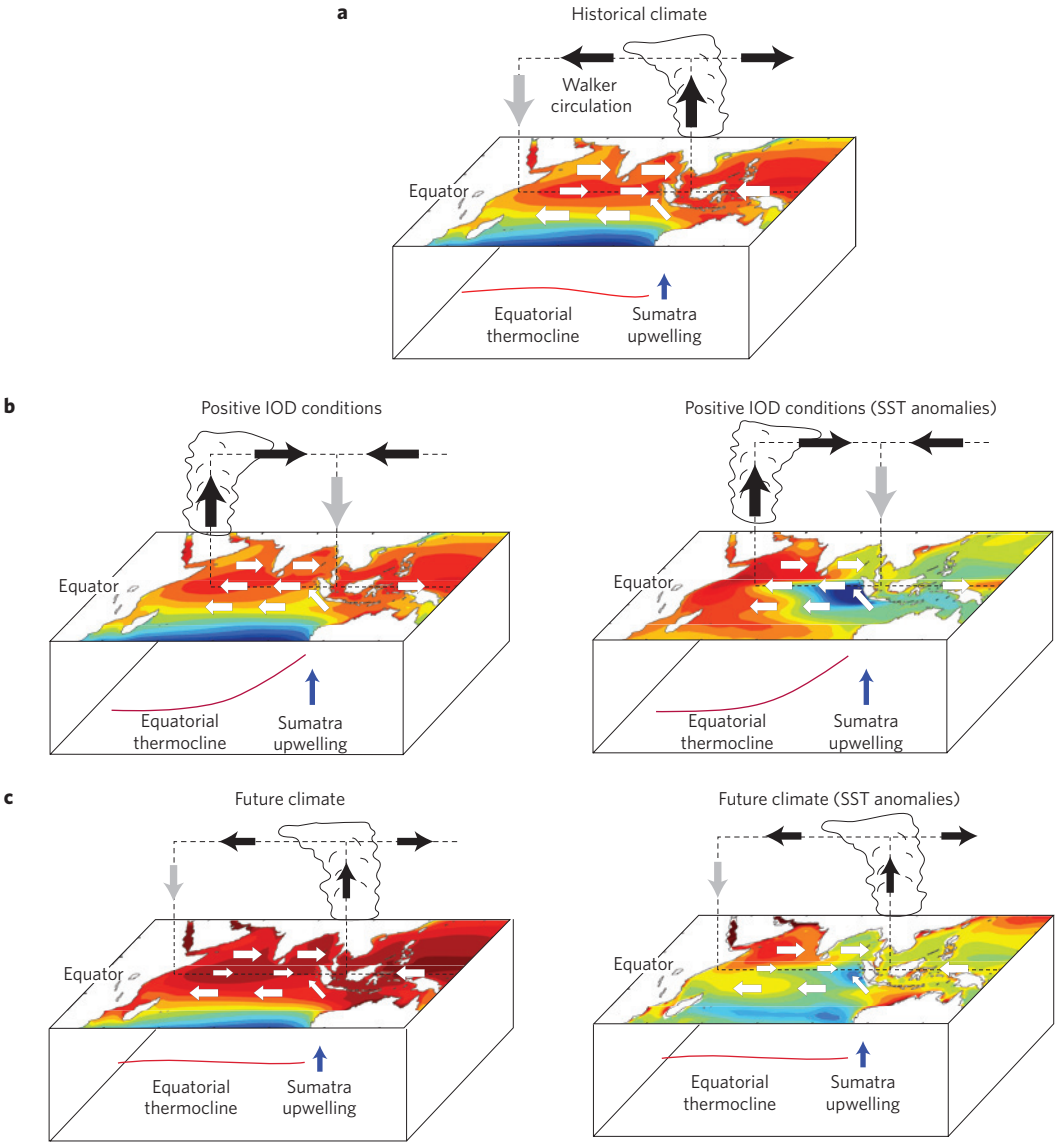

Figure 2 | Historical austral spring mean climate and positive IOD conditions for the twentieth century, and future austral spring mean climate. **a**, Historical mean climate, indicating SSTs, surface winds, the associated Walker circulation, the mean position of convection and the thermocline. In the western Indian Ocean, the descending branch is broad and not well-defined, as indicated by a grey arrow. **b**, Typical conditions during a positive IOD event. **c**, Projected future mean climate based on a CMIP5 multi-model ensemble average[57]. Diagrams with total SST fields are shown on the left; diagrams with SST anomalies referenced to the 1961–1999 mean for **b**, and referenced to the basin mean for **c**, are shown on the right.

This hydrological cycle mechanism is muted with respect to the available moisture increase, and therefore means that the Walker circulation weakening could occur without a well-defined change in the zonal SST gradient[72,73]. However, recent modelling and observational results indicate that the weakened Walker circulation over the past six decades (1950–2009) can be attributed to an observed SST warming pattern characterized by a weakening in the west-minus-east SST gradient in the Indo-Pacific[67], which suggests a coupling between oceanic and atmospheric changes. This seems to be the case in future climate simulations from CGCMs (ref. 55).

The zonally asymmetric Indian Ocean Walker circulation (shown schematically in Fig. 2) is a useful illustration of the atmospheric vertical overturning. The eastern tropical Indian Ocean forms part of the warm pool with the warmest SSTs on Earth that supports the rising branch of the broader Indo-Pacific Walker circulation. Under normal austral spring conditions, total SSTs in the eastern Indian and western Pacific warm pool are higher than those in the western Indian Ocean, and the thermocline is slightly deeper in the east than the west (Fig. 2a)[74]. Equatorial westerlies flow over the northern equatorial Indian Ocean, converging at the warm pool. The south-easterlies off the Sumatra–Java coast and over the southern tropical Indian Ocean are weakly linked with the Walker circulation. During pIOD events, anomalous cooling over the southeastern equatorial Indian Ocean is accompanied by anomalous warming in the west, such that in the meridional direction the warmest water is located in the northeastern Indian Ocean. However, in the zonal direction along the equatorial Indian Ocean, warmest SSTs are located to the west, leading to a reversal of the Walker circulation with the rising branch in the west (Fig. 2b, total SSTs in the left panel, SST anomalies in the right). Under greenhouse warming, CGCMs simulate a reduction in the vertical atmospheric circulation. Although uncertainty remains, the reduction would mean a weakening of the equatorial westerlies, or a relative strengthening of the equatorial easterlies, that feed the rising branch of the Walker circulation, which is simulated to be located in the same position as in the present-day climate (Fig. 2c).

In CGCMs, the relative strengthening of the equatorial easterlies drives a series of changes in the mean oceanic circulation: the thermocline shallows in the eastern Indian Ocean, and wind-induced seasonal equatorial upwelling Kelvin waves propagate eastwards to Sumatra–Java. This leads to a relatively weak warming trend in the eastern Indian Ocean compared to the west, and a further strengthening of the equatorial easterlies. These changes are consistent with the feedback described by Bjerknes[31], which is widely recognised as the fundamental process for the IOD (see Box 1) on interannual time scales[32–37]. Thus, under global warming, the adjustment in the Indian Ocean produces dynamical responses in equatorial winds, SSTs and the thermocline over the eastern Indian Ocean that are in accordance with the Bjerknes feedback, as found in the Pacific[73]. Much of the relatively weak warming in the eastern Indian Ocean, particularly off Sumatra–Java, is induced by the equatorial easterly wind trends. There is little change in winds off Sumatra–Java.

The term 'pIOD-like climate change' seems appropriate when describing the mean change in the tropical Indian Ocean, as the reduction in the strength of the equatorial winds under climate change is accompanied by a well-defined increase in the west-minus-east SST gradient. However, the mean future Indo-Pacific Walker circulation structure is rather different from that during pIODs in terms of the position of the convection centre. Therefore, such an analogy could potentially confuse the fact that future IOD events will continue to occur within a background mean Walker circulation that resembles present-day conditions.

The projected future mean circulation changes of the tropical Indian Ocean described above are physically consistent, despite the fact that recent observational studies[69] cast doubt on such modelled results[70,71]. There are many model biases in the representation of the present-day climate. CGCMs systematically simulate a thermocline that slopes upwards towards the eastern Indian Ocean (opposite to what is observed), a west-minus-east mean SST gradient that is stronger than that observed, equatorial easterlies that are too strong, and an IOD amplitude that is too large[74]. These biases have a direct bearing on simulated IOD events and future climate projections in IOD-affected regions — and in some CGCMs, the biases are comparable in magnitude with, or even larger than, the projected anthropogenic climate change signals[75]. Another aspect of model bias is an unrealistically weak relationship with ENSO (refs 52,75). It is unknown whether these model deficiencies, particularly the reversed slope of the mean thermocline, influence the details of mean changes in climate. Nevertheless, given the robustness of the modelled weakening Walker circulation, and the associated equatorial easterly wind trend, which lifts the thermocline in the eastern Indian Ocean, it is expected that these mean changes are qualitatively robust.

The response of the IOD to global warming

One way of examining the sensitivity of tropical variability to climate change is to study the past history of variability using proxy-based climate reconstructions. For the IOD, only limited reconstructions are available. Coral geochemical records over the past 6,500 years from the Mentawai Islands (near Java) show that pIOD events during the early middle Holocene were characterized by a longer duration of strong near-surface ocean cooling than in the present-day climate, indicative of IOD-related drought periods in the eastern tropical Indian Ocean[24]. During this period, there was a broad-scale strengthening of the Asian summer monsoon owing to increased Northern Hemisphere summer insolation[76], ENSO variability was suppressed[77,78], and the mean state of the tropical Pacific Ocean was characterized by an enhanced west-minus-east SST gradient[79,80]. Meanwhile, the Indian Ocean SSTs were cooler in the east than in the west[24]. The prolonged cooling during pIOD events was due to an early development of anomalous Ekman upwelling in the eastern Indian Ocean sector associated with stronger cross-equatorial winds driven by enhanced boreal summer warming of the Asian landmass. Under global warming, the strength of Asian monsoons has been predicted to increase[81,82], with enhanced equatorial easterlies consistent with a weakening Walker circulation and intensifying monsoon. This projected intensification of the monsoon has not been observed so far; in fact, Asian summer monsoon has weakened since the 1950s[83]. Despite this, the increased west-minus-east SST gradient along the equatorial Indian Ocean and stronger Asian monsoons of the early middle Holocene may arguably provide an analogy to the greenhouse scenario. However, under greenhouse conditions there is no consensus on the change of El Niño amplitude[72].

Another difficulty in detecting externally forced changes in the IOD properties using observations lies in the large intrinsic variations in ENSO (ref. 84), the monsoon and their relationship, which can occur on multi-decadal to centennial timescales, even in the absence of an external forcing[85–87]. Such naturally occurring variability might be masking greenhouse-warming-induced changes in the IOD. This issue can be partially addressed in CGCMs by performing multiple runs with the same model[62] measuring forced changes against natural variability from long unforced control experiments, and using multiple CGCMs forced with future global warming emission scenarios[57]. A multi-model ensemble average strongly reduces natural variability, which is independent from model to model, leaving changes predominantly induced by greenhouse warming.

The future IOD amplitude and frequency above the time-varying mean state do not show a significant change. Some CGCMs generate an increase in the amplitude and/or frequency of IOD variability in the twenty-first century, whereas some show a decrease, but most changes are not statistically significant (Fig. 3a,b). This null result can mask changes in the associated feedbacks. Given the change in the mean circulation, it is possible to assess the response of individual feedbacks and processes, and elucidate how the IOD characteristics might be impacted. Our examination below focuses on the IOD peak season, austral spring.

Seasonal phase locking. The majority of CGCMs show that pIOD events will continue to develop and mature in the months from June to November[52,53,55]. In observations, there is some indication that a new type of pIOD is emerging. This new type develops and terminates earlier than a classical pIOD, due to a weakening Indian Ocean Walker circulation, or an earlier onset of the Asian summer monsoon[88]. Whether such pIOD events are captured by CGCMs remains unclear, although a set of 'reasonable' models with the strongest land–sea thermal contrast does suggest an earlier onset of the Asian summer monsoon[89]. An early Asian summer monsoon onset means an early commencement of easterlies over Sumatra–Java, which could facilitate early development of a pIOD. Further, the majority of CGCMs also simulate a delayed Australian monsoon onset with an associated reduction in the westerlies[90,91], suggesting a prolonged season for development of pIODs.

Thermocline–SST feedback. Changes to the eastern Indian Ocean thermocline depth and to the east-to-west thermocline slope can influence the characteristics of the IOD. The climatological thermocline shallows in CGCMs under greenhouse warming, because of enhanced long-term mean easterlies over Sumatra–Java and along the equatorial Indian Ocean, with a faster warming rate near the surface. Because of the shoaling[63], the SST response to thermocline should increase[55]. This is seen in the majority of CGCMs and in the PPE experiments (Fig. 3c), and is expected to enhance the amplitude of IOD events.

Zonal wind and zonal SST gradient feedback. Under greenhouse warming, the atmospheric air column becomes more stable as the troposphere tends to warm at a faster rate than the surface[92,93]. This is expected to weaken the atmospheric component of the Bjerknes feedback. In the majority of CGCMs and PPE experiments, the

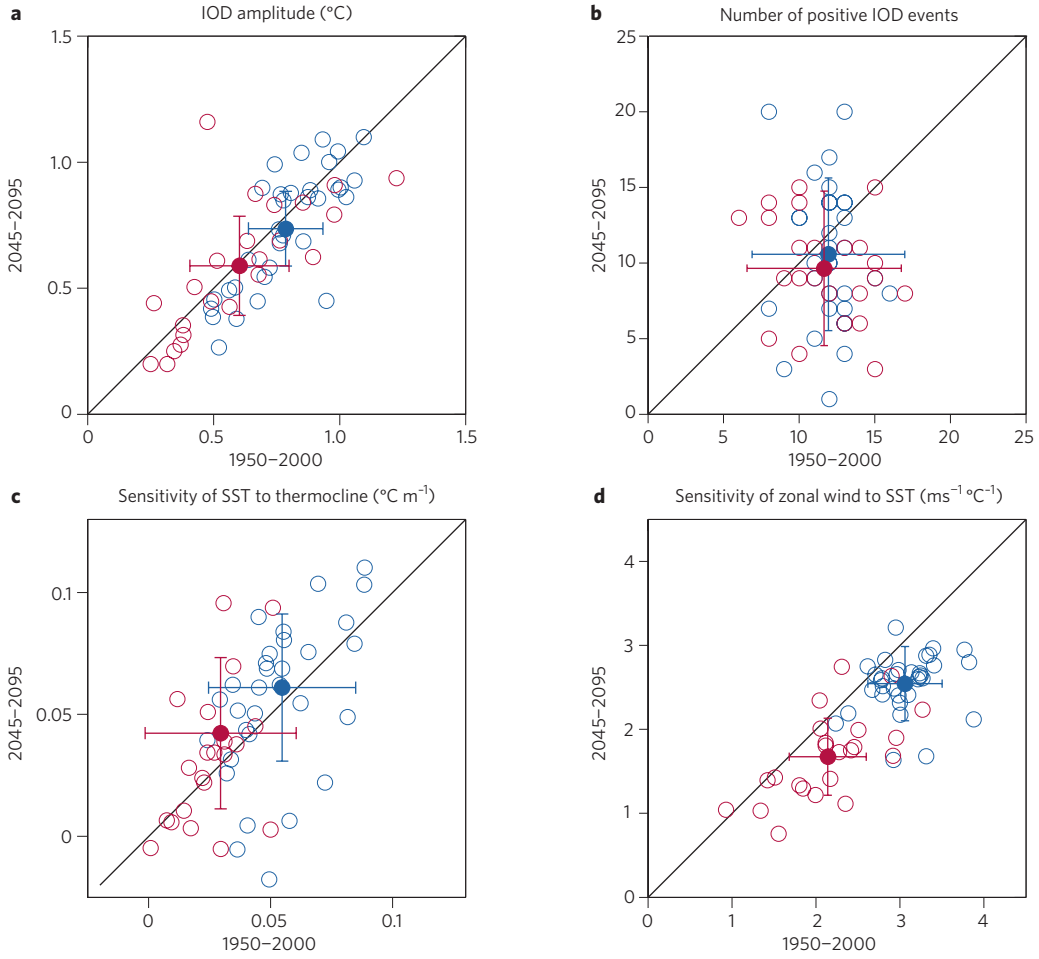

Figure 3 | Projected changes in the IOD characteristics and associated ocean–atmosphere feedback strengths. Red and blue circles are from the CMIP5 multi-model ensemble[57] and the perturbed physics ensemble[62], respectively. Filled circles with error bars show the multi-model average and the inter-model standard deviation. **a**, IOD amplitude (DMI standard deviation, °C). **b**, The number of positive IOD events. **c**, The response of SST in the eastern equatorial Indian Ocean to local thermocline depth. **d**, The response of central equatorial wind to an SST anomaly in the eastern equatorial Indian Ocean[55]. Each panel shows calculations for historical (1950–2000) and future (2045–2095) periods.

increased stability leads to a decreased sensitivity of zonal winds over the equatorial Indian Ocean to zonal SST gradients (Fig. 3d), and is accompanied by a reduced variance in zonal winds and the thermocline depth[55]. This change is expected to weaken the amplitude of the IOD.

Surface zonal advective feedback. Anomalous east-to-west advection of the mean SST gradient amplifies pIOD events. It is not clear if or how this positive feedback may be affected by the CGCM bias; the majority of CGCMs simulate a climatological west-minus-east SST gradient that is stronger than the observed negative gradient[74]. Under climate change, the mean west-minus-east SST gradient strengthens. However, because the variance of zonal currents decreases in response to reduced zonal wind variability, a likely outcome is that this feedback would not change significantly under climate change, as it involves two offsetting factors.

SST–cloud–radiation feedback. As a part of the reduced atmospheric feedback, the response of precipitation and cloud to variability of SST over the eastern tropical Indian Ocean weakens in the majority of CGCMs, with a decreased response in shortwave radiation. The decreased precipitation and cloud response is accompanied by a reduced variance of precipitation. This, in turn, is due to a decrease in climatological rainfall over the eastern tropical Indian Ocean, governed by a dynamical adjustment to a slower warming rate in the eastern tropical Indian Ocean than in the west[72]. The majority of CGCMs also project a decreased atmospheric circulation response to anomalous heating, indicated by a weaker response of zonal winds to rainfall variations. Cloud feedbacks and their link to subsidence and convection remain a large uncertainty in CGCMs[94].

Wind–evaporation–SST feedback. During the early development of a pIOD event, stronger-than-normal easterly winds superimpose on long-term mean easterly winds, enhancing evaporative cooling — which is conducive to cool SST anomalies over Sumatra–Java, acting as a positive feedback. This process is likely to commence early, with an early onset of the Asian summer monsoon[89]. The switch to a negative feedback, when the easterly wind anomalies superimpose on climatological westerly winds, is likely to occur later in association with a later onset of the Australian summer monsoon[90,91]. It is expected that the strong seasonality of this feedback will continue. The intensity of this feedback, however, may not undergo a significant change because an impact from increased climatological SSTs that favour a strengthening intensity is offset by decreased easterly wind variability.

Forcing by ENSO. As the IOD interacts with ENSO[25–28,30], a change in ENSO amplitude under greenhouse warming may induce a change in IOD amplitude. To date, there is no consensus on how ENSO will respond to greenhouse warming[72]. The relationship between the IOD and ENSO is generally weaker in CGCMs (refs 52,75) than

is indicated by observations over the past 60 years, and there is no statistically significant inter-model relationship between the change in the IOD amplitude and ENSO amplitude change[55]. Thus, there is no evidence supporting an IOD amplitude change as a consequence of ENSO's response to greenhouse warming.

IOD skewness. The amplitude of pIOD events tends to be greater than that of nIOD events, and this is referred to as the positive amplitude skewness. One of the fundamental reasons for this skewness is a deep thermocline in the eastern Indian Ocean. A further deepening induces only a small surface warming, in contrast to a shallowing thermocline that is more effective in generating a surface cooling[43,44]. Under greenhouse warming, as the climatological thermocline shoals, there is a tendency for a reduced skewness (Fig. 4) in the majority of CGCMs with an averaged reduction of 40%, and in PPE experiments. As the climatological thermocline shoals, any anomalous deepening of the thermocline on an interannual time scale becomes more effective in generating a surface warming anomaly. In association, asymmetry in the thermocline-SST feedback between a shoaling and a deepening thermocline weakens.

Nonlinear dynamical heating. Advection of anomalous zonal (vertical) temperature gradients in the upper layers of the eastern Indian Ocean by anomalous zonal (vertical) currents gives rise to a temperature tendency that reinforces cool anomalies off Sumatra–Java during pIOD events, but dampens warm anomalies during nIOD events, contributing to the amplitude skewness[41,43]. Under greenhouse warming, a combination of no significant change in variability of zonal temperature gradients and reduced variability of zonal currents could contribute to decreased nonlinear dynamical heating. However, it is less clear how variability of the vertical temperature gradient and vertical velocities, as well as their product, will change in a shoaling thermocline environment. Thus the net impact to this process needs to be further examined.

Other processes. Other factors have been shown to play a role in the IOD life cycle and characteristics. One such factor is a modulation by decadal variability[95], which a multi-model ensemble average effectively eliminates, and is not discussed here. Another factor arises from the prominent feature of a large freshwater input from the Bay of Bengal and the Indonesian Throughflow to the eastern tropical Indian Ocean[96]. This freshwater flux favours a salinity-stratified intermediate layer between the base of the mixed layer and the top of the thermocline, a depth range referred to as a barrier layer[97], which is quasi-permanent off the Sumatra coast and comprises a semi-annual cycle with a maximum in November. The barrier layer has an impact on the IOD (ref. 98): during pIOD events, thinning of the barrier layer occurs, strengthening the associated air–sea interactions[99,100]. Under greenhouse warming, the isothermal layer and climatological rainfall off Sumatra–Java are expected to decrease, with a tendency to reduce the mean barrier layer. However, we do not know how the input of freshwater from the Bay of Bengal and the Indonesian Throughflow, or how the pre-austral winter salt transport to the Sumatra waters, will change. Further research is required on how barrier layer variability and its relationship with the IOD will evolve.

It is evident that under future greenhouse warming, some characteristics, processes and feedbacks of the IOD are likely to change in association with changes in the mean climate. Consensus among CGCMs is particularly high in terms of a strengthening of the thermocline–SST feedback and a reduced atmospheric feedback with a reduced response of zonal winds to zonal SST gradients. For other feedbacks (for example, wind–evaporation–SST feedback and nonlinear dynamical heating) there is either little overall change or currently no evidence to suggest that they will change substantially. The net effect from offsetting changes in the feedbacks is that variability of the IOD, referenced to an evolving mean state, is not expected to change substantially. However, it is likely that the IOD skewness will decrease (Fig. 4), although not all processes that might contribute to this change are understood.

Uncertainty behind the CGCM consensus

The mean climate of the tropical Indian Ocean will continue to change throughout the twenty-first century as a result of past and future projected emissions of greenhouse gases. The consensus seems high among CGCMs: the atmosphere will become more stable, climatological zonal easterly winds over the southern equatorial Indian Ocean will strengthen, the SST change is likely to feature a slower warming rate in the east than in the west, and the thermocline off Sumatra–Java is likely to shoal. The feedbacks that control the characteristics of the IOD are likely to be affected by these changes, but the change in the IOD intensity is determined by a balance between amplifying and dampening processes, or weakening and strengthening positive feedbacks. The majority of CGCMs suggest that variability of the IOD will undergo little change when referenced to the time-evolving mean climate described above. However, when referenced to a fixed-period climatology of past decades, the slower warming rate in the east than the west manifests as increased occurrences of pIOD events, a feature statistically consistent with what has been observed over the late twentieth century.

Behind the relatively high level of consensus, there are a number of systematic biases in the CGCMs which could be sources of uncertainties. The IOD can be influenced by ENSO and the Asian summer monsoon, but changes in ENSO and the monsoon are themselves uncertain. Most importantly, the majority of CGCMs simulate an easterly mean wind direction over the equatorial Indian Ocean,

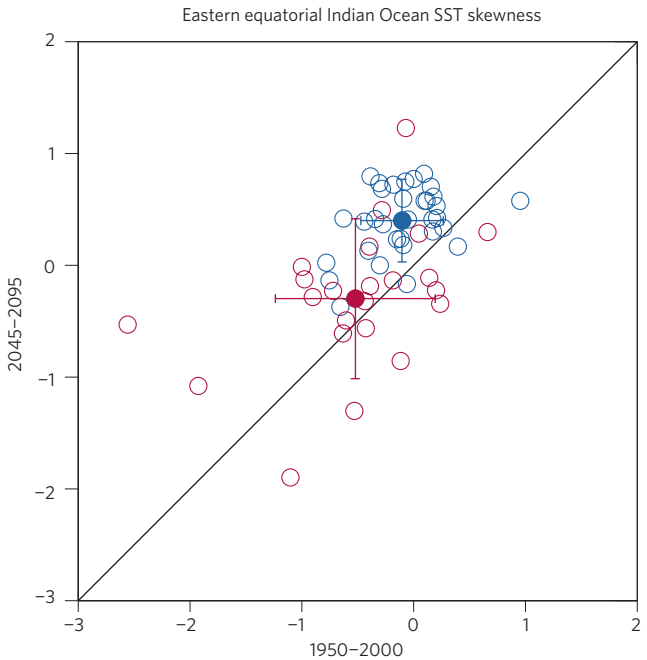

Figure 4 | Projected changes in SST skewness of the eastern equatorial Indian Ocean. Shown are calculated using anomalies referenced to a time-evolving mean state climate. Skewness is defined as a measure of the asymmetry of a probability distribution function, calculated for present-day (1950–2000) and future (2045–2095) periods[55]. Red and blue circles are values derived from the CMIP5 multi-model ensemble[57] and the perturbed physics ensemble[62], respectively. Filled circles with error bars show the multi-model average and the inter-model standard deviation. There is a tendency for the skewness to decrease in the future climate.

warmer SSTs in the western than in the eastern equatorial basin in the long-term average, and a thermocline that slopes upwards towards the east — all of which are unrealistic features. We do not know their impact, but such biases may affect the strength and balance of the feedbacks that determine the characteristics of the IOD under greenhouse warming. CGCMs simulate an IOD amplitude that is, on average, approximately twice as large as that observed[74], indicating that at least some elements of the Bjerknes feedback are too strong, or the balance of amplifying and damping feedbacks is skewed towards an overly large amplifying effect. Perturbed by circulation changes in response to greenhouse warming, the overly strong net amplifying effect could produce a response in the mean climate that is systematically too large.

Indeed, inter-model statistics reveal that CGCMs with a greater mean west-to-east upward thermocline slope tend to simulate stronger positive feedbacks and a larger IOD amplitude[74]. In turn, models with a greater IOD amplitude systematically produce a greater change in mean rainfall and surface temperature in IOD-affected regions under global warming[75]. These findings suggest that a realistic simulation of the mean climate of the Indian Ocean and the statistical properties of the IOD are essential for accurate climate projections. Reversely, current climate projections in IOD-affected regions carry considerable uncertainties because of the biases in CGCMs.

Given these uncertainties, it may be several more years before a set of reliable climate change projections for IOD-affected regions can be developed. One approach would be to select a subset of CGCMs that simulate a realistic IOD amplitude. However, unfortunately, the models that are closest to observations in terms of IOD amplitude tend to perform not well in terms of simulating the observed IOD pattern, the relationship of the IOD with other tropical modes of variability, and the tropical modes of variability themselves[75]. Future efforts should focus on improving CGCM simulation of the strength of various feedback processes and their balance, particularly the feedbacks between the thermocline and SSTs and between zonal winds and zonal SST gradients, to understand future changes in the properties of the IOD — and ultimately climate.

Received 14 may 2013; accepted 18 october 2013; published online 28 November 2013

References

1. Le Treut, H. *et al.* in *Climate Change 2007: The Physical Science Basis* (eds. Solomon, S. *et al.*) 19–20 (Cambridge University Press, 2007).
2. Gleckler, P. J. *et al.* Human-induced global ocean warming on multidecadal timescales. *Nature Clim. Change* **2,** 524–529 (2012).
3. Alory, G., Wijffels, S. & Meyers, G. Observed temperature trends in the Indian Ocean over 1960–1999 and associated mechanisms. *Geophys. Res. Lett.* **34,** L02606 (2007).
4. Saji, N. H., Goswami, B. N., Vinayachandran, P. N. & Yamagata, T. A dipole in the tropical Indian Ocean. *Nature* **401,** 360–363 (1999).
5. Webster, P. J., Moore, A. M., Loschnigg, J. P. & Leben, R. R. Coupled oceanic-atmospheric dynamics in the Indian Ocean during 1997–98. *Nature* **401,** 356–360 (1999).
6. Yu, L. & Rienecker, M. M. Mechanisms for the Indian Ocean warming during the 1997–98 El Niño. *Geophys. Res. Lett.* **26,** 735–738 (1999).
7. Murtugudde, R., McCreary, J. P. & Busalacchi, A. J. Oceanic processes associated with anomalous events in the Indian Ocean with relevance to 1997–1998 *J. Geophys. Res*. **105,** 3295–3306 (2000).
8. Cai, W., Cowan, T. & Sullivan, A. Recent unprecedented skewness towards positive Indian Ocean Dipole occurrences and its impact on Australian rainfall. *Geophys. Res. Lett*. **36,** L11705 (2009).
9. Ihara, C., Kushnir, Y. & Cane, M. A. Warming trend of the Indian Ocean SST and Indian Ocean Dipole from 1880 to 2004. *J. Clim*. **21,** 2035– 2046 (2008).
10. Abram, N. J., Gagan, M. K., Cole, J. E., Hantoro, W. S. & Mudelsee, M. Recent intensification of tropical climate variability in the Indian Ocean. *Nature Geosci*. **1,** 849–853 (2008).
11. Kripalani, R. H., Oh, J. H. & Chaudhari, H. S. Delayed influence of the Indian Ocean Dipole mode on the East Asia–West Pacific monsoon: possible mechanism. *Int. J. Climatol.* **30,** 197–209 (2010).
12. Ashok, K., Guan, Z. & Yamagata, T. Influence of the Indian Ocean Dipole on the Australian winter rainfall. *Geophys. Res. Lett.* **30,** L1821 (2003).
13. Meyers, G. A., McIntosh, P. C., Pigot, L. & Pook, M. J. The years of El Niño, La Niña, and interactions with the tropical Indian Ocean. *J. Clim.* **20,** 2872–2880 (2007).
14. Ummenhofer, C. C. *et al.* What causes southeast Australia's worst droughts? *Geophys. Res. Lett*. **36,** L04706 (2009).
15. Zubair, L., Rao, S. A. & Yamagata, T. Modulation of Sri Lankan Maha rainfall by the Indian Ocean dipole. *Geophys. Res. Lett.* **30,** 1063 (2003).
16. Behera, S. K. *et al.* Paramount impact of the Indian Ocean Dipole on the East African short rains: A CGCM study. *J. Clim.* **18,** 4514–4530 (2005).
17. Black, E., Slingo, J. & Sperber, K. R. An observational study of the relationship between excessively strong short rains in coastal East Africa and Indian Ocean SST. *Mon. Weather Rev.* **131,** 74–94 (2003).
18. Ashok, K., Guan, Z. & Yamagata, T. Impact of the Indian Ocean dipole on the relationship between the Indian monsoon rainfall and ENSO. *Geophys. Res. Lett.* **28,** 4499–4502 (2001).
19. Cai, W., Cowan, T. & Raupach, M. Positive Indian Ocean Dipole events precondition southeast Australia bushfires. *Geophy. Res. Lett.* **36,** L19710 (2009).
20. Abram, N. J., Gagan, M. K., McCulloch, M. T., Chappell, J. & Hantoro, W. S. Coral reef death during the 1997 Indian Ocean Dipole linked to Indonesian wildfires. *Science* **301,** 952–955 (2003).
21. Hashizume, M., Chaves, L. F. & Minakawa, N. Indian Ocean Dipole drives malaria resurgence in East African highlands. *Sci. Rep.* **2,** 269 (2012).
22. Tokinaga, H. & Tanimoto, Y. Seasonal transition of SST anomalies in the tropical Indian Ocean during El Niño and Indian Ocean Dipole years. *J. Meteorol. Soc. Japan* **82,** 1007–1018 (2004).
23. Fischer, A., Terray, P., Guilyardi, E., Gualdi, S. & Delecluse, P. Two independent triggers for the Indian Ocean Dipole/Zonal Mode in a coupled GCM. *J. Clim*. **18,** 3428–3449 (2005).
24. Abram, N. J. *et al.* Seasonal characteristics of the Indian Ocean Dipole during the Holocene epoch. *Nature* **445,** 299–302 (2007).
25. Annamalai, H., Xie, S. -P., McCreary, J. P. & Murtugudde, R. Impact of Indian Ocean sea surface temperature on developing El Niño. *J. Clim.* **18,** 302–319 (2005).
26. Yuan, D. *et al.* Forcing of the Indian Ocean Dipole on the interannual variations of the tropical Pacific Ocean: roles of the Indonesian Throughflow. *J. Clim,* **24,** 3593–3608 (2011).
27. Luo, J. J. *et al.* Interaction between El Niño and Extreme Indian Ocean Dipole. *J. Clim*. **23,** 726–742.
28. Izumo T. *et al.* Influence of the state of the Indian Ocean Dipole on the following year's El Niño. *Nature Geosci*. **3,** 168–172 (2010).
29. Saji, N. H. & Yamagata, T. Possible impacts of Indian Ocean Dipole mode events on global climate. *Clim. Res.* **25,** 151–169 (2003).
30. Cai, W., van Rensch, P., Cowan, T. & Hendon, H. H. Teleconnection pathways of ENSO and the IOD and the mechanisms for impacts on Australian rainfall. *J. Clim.* **24,** 3910–3923 (2011).
31. Bjerknes, J. Atmospheric teleconnections from the equatorial Pacific. *Mon. Weather Rev*. **97,** 163–172 (1969).
32. Reverdin, G., Cadel, D. & Gutzler, D. Interannual displacements of convection and surface circulation over the equatorial Indian Ocean. *Q. J. R. Meteorol. Soc.* **112,** 43–67 (1986).
33. Hastenrath, S., Nicklis, A. & Greischar, L. Atmospheric-hydrospheric mechanisms of climate anomalies in the western equatorial Indian Ocean. *J. Geophys. Res.* **98,** 20219–20235 (1993).
34. Udea, H. & Matsumoto, J. A. Possible triggering process of east–west asymmetric anomalies over the Indian Ocean in relation to 1997/1998 El Niño. *J. Meteor. Soc. Japan* **78,** 803–818 (2000).
35. Xie, S.-P., Annamalai, H., Schott, F. & McCreary, J. P. Jr. Origin and predictability of South Indian Ocean climate variability. *J. Clim*. **15(8)**, 864–874 (2002).
36. Annamalai, H., Murtugudde, R. Wang, B. Potemra, J. & Xie, S-P. Coupled dynamics in the Indian Ocean: spring initiation of the zonal mode. *Deep Sea Res. II* **50,** 2305–2330 (2003).
37. Murtugudde, R. & Busalacchi, A. J. Interannual variability of the dynamics and thermodynamics, and mixed layer processes in the Indian Ocean. *J. Clim.* **12,** 2300–2326 (1999).
38. Li, T., Zhang, Y. S., Chang, C-P., Lu, E. & Wang, D. Relative role of dynamic and thermodynamic processes in the development of the Indian Ocean dipole: An OGCM diagnosis. *Geophys. Res. Lett*. **29,** 2110 (2002).
39. Li, T., Wang, B., Chang, C-P. & Zang, Y. A theory for the Indian Ocean dipole–zonal mode. *J. Atmos. Sci*. **60,** 2119–2135 (2003).
40. Shinoda, T., Alexander, M. A. & Hendon, H. H. Remote response of the Indian Ocean to interannual SST variations in the tropical Pacific. *J. Clim.* **17,** 362–372 (2004).
41. Hong, C. C., Li, T., Lin, H. & Kug, J. S. Asymmetry of the Indian Ocean Dipole. Part I: Observational Analysis. *J. Clim.* **21,** 4834–4848 (2008).
42. Hong, C. C. & Li, T. Independence of SST skewness from thermocline feedback in the eastern equatorial Indian Ocean. *Geophys. Res. Lett*. **37,** L11702 (2010).

43. Cai, W. & Qiu, Y. An observation-based assessment of nonlinear feedback processes associated with the Indian Ocean Dipole. *J. Clim.* **26,** 2880–2890 (2013).
44. Ogata, T., Xie, S.-P., Lan, J. & Zheng, X. Importance of ocean dynamics for the skewness of the Indian Ocean Dipole mode. *J. Clim.* **26,** 2145–2159 (2013).
45. Iizuka, S., Matsuura, T. & Yamagata, T. The Indian Ocean SST dipole simulated in a coupled general circulation model. *Geophys. Res. Lett.* **27,** 3369–3372 (2000).
46. Baquero-Bernal, A., Latif, M. & Legutke, S. On dipole-like variability of sea surface temperature in the tropical Indian Ocean. *J. Clim.* **15,** 1358–1368 (2002).
47. Yu, J.-Y., Mechoso, C. R., McWilliams, J. C. & Arakawa, A. Impacts of the Indian Ocean on the ENSO cycle. *Geophys. Res. Lett.* **29,** 1204 (2002).
48. Loschnigg, J., Meehl, G. A., Webster, P. J., Arblaster, J. M. & Compo, G. P. The Asian monsoon, the Tropospheric Biennial Oscillation, and the Indian Ocean Zonal Mode in the NCAR CSM. *J. Clim.* **16,** 1617–1642 (2003).
49. Gualdi, S., Guilyardi, E., Navarra, A., Masina, S. & Delecluse, P. The interannual variability in the tropical Indian Ocean as simulated by a CGCM. *Clim. Dyn.* **20,** 567–582 (2003).
50. Lau, N-C. & Nath, M. J. Coupled GCM simulation of atmosphere–ocean variability associated with zonally asymmetric SST changes in the tropical Indian Ocean. *J. Clim.* **17,** 245–265 (2004).
51. Spencer, H., Sutton, R. T., Slingo, J. M., Roberts, M. & Black, E. Indian Ocean climate and dipole variability in Hadley Centre coupled GCMs. *J. Clim.* **18,** 2286–2306 (2005).
52. Saji, N. H., Xie, S-P. & Yamagata, T. Tropical Indian Ocean variability in the IPCC 20th-century climate simulations. *J. Clim.* **19,** 4397–4417 (2006).
53. Cai, W., Sullivan, A. & Cowan, T. Interactions of ENSO, the IOD, and the SAM in CMIP3 models. *J. Clim.* **24,** 1688–1704 (2010).
54. Liu, L., Yu, W. & Li, T. Dynamic and thermodynamic air-sea coupling associated with the Indian Ocean Dipole diagnosed from 23 WCRP CMIP3 models. *J. Clim.* **24,** 4941–4958 (2011).
55. Zheng, X. T. *et al.* Indian Ocean Dipole response to global warming in the CMIP5 multimodel ensemble. *J. Clim.* **26,** 6067–6080 (2013).
56. Meehl, G. *et al.* The WCRP CMIP3 multimodel Dataset: A New Era in Climate Change Research. *Bull. Am. Meteorol. Soc.* **88,** 1383–1394 (2007).
57. Taylor, K. E., Stouffer, R. J. & Meehl, G. A. An overview of CMIP5 and the experimental design. *Bull. Am. Meteorol. Soc.* **93,** 485–498 (2012).
58. Rayner, N. A. *et al.* Global analyses of sea surface temperature, sea ice, and night marine air temperature since the late nineteenth century. *J. Geophys. Res.* **108,** 4407 (2003).
59. Ishii, M. & Kimoto, M. Reevaluation of historical ocean heat content variations with time-varying XBT and MBT depth bias corrections. *J. Oceanogr.* **65,** 287–299 (2009).
60. Smith, T. M. & Reynolds, R. W. Improved extended reconstruction of SST (1854–1997). *J. Clim.* **17,** 2466–2477 (2004).
61. Alley, R. *et al. Climate change 2007: The physical science basis, summary for policymakers* (World Meteorol. Org., 2007).
62. Collins, M. *et al.* A comparison of perturbed physics and multi-model ensembles: Model errors, feedbacks and forcings. *Clim. Dyn.* **36,** 1737–1766 (2011).
63. Vecchi, G. A. & Soden, B. J. Global warming and the weakening of the tropical circulation. *J. Clim.* **20,** 4316–4340 (2007).
64. Vecchi, G. A. *et al.* Weakening of tropical Pacific atmospheric circulation due to anthropogenic forcing. *Nature* **441,** 73–76 (2006).
65. Held, I. M. & Soden, B. J. Robust responses of the hydrological cycle to global warming. *J. Clim.* **19,** 5686–5699 (2006).
66. Allen, M. R. & Ingram, W. J. Constraints on future changes in climate and the hydrologic cycle. *Nature* **419,** 224–232 (2002).
67. Tokinaga, H., Xie, S-P., Deser, C., Kosaka, Y. & Okumura, Y. M. Slowdown of the Walker circulation driven by tropical Indo-Pacific warming. *Nature* **491,** 439–443 (2012).
68. Dong, B. W. & Lu, R. Y. Interdecadal enhancement of the Walker circulation over the Tropical Pacific in the late 1990s. *Adv. Atmos. Sci.* **30,** 247–262 (2013).
69. Solomon, A. & Newman, M. Reconciling disparate twentieth-century Indo-Pacific ocean temperature trends in the instrumental record. *Nature Clim. Change* **2,** 691–699 (2012).
70. L'Heureux, M., Lee, S. & Lyon, B. Recent multidecadal strengthening of the Walker circulation across the tropical Pacific. *Nature Clim. Change* **3,** 571–576 (2013).
71. Newman M. Winds of change. *Nature Clim. Change* **3,** 538–539 (2013).
72. Xie, S-P. *et al.* Global warming pattern formation: sea surface temperature and rainfall. *J. Clim.* **23,** 966–986 (2010).
73. Collins, M. *et al.* The impact of global warming on the tropical Pacific Ocean and El Niño. *Nature Geosci.* **3,** 391–397 (2010).
74. Cai, W. & Cowan, T. Why is the amplitude of the Indian Ocean Dipole overly large in CMIP3 and CMIP5 climate models? *Geophys. Res. Lett.* **40,** 1200–1205 (2013).
75. Weller, E. & Cai, W. Realism of the Indian Ocean Dipole in CMIP5 models: the implication for climate projections. *J. Clim.* **26,** 6649–6659 (2013).
76. Yuan, D. *et al.* Timing, duration, and transitions of the Last Interglacial Asian monsoon. *Science* **304,** 575–578 (2004).
77. Moy, C. M., Seltzer, G. O., Rodbell, D. T. & Anderson, D. M. Variability of El Niño/Southern Oscillation activity at millennial timescales during the Holocene epoch. *Nature* **420,** 162–165 (2002).
78. Tudhope, A. W., Chilcott, C. P. & McCulloch, M. T. Variability in the El Niño-Southern oscillation through a glacial-interglacial cycle. *Science* **291,** 1511–1517 (2001).
79. Koutavas, A., Lynch-Stieglitz, J., Marchitto, T. M. & Sachs, J. P. El Niño-like pattern in Ice Age tropical Pacific sea surface temperature. *Science* **297,** 226–230 (2002).
80. Liu, Z., Brady, E. & Lynch-Stieglitz, J. Global ocean response to orbital forcing in the Holocene. *Paleoceanography* **18,** 1041 (2003).
81. Ashrit, R. G., Kumar, K. R. & Kumar, K. K. ENSO–monsoon relationships in a greenhouse warming scenario. *Geophys. Res. Lett.* **28,** 1727–1730 (2001).
82. Zickfeld, K., Knopf, B., Petoukhov, V. & Schellnhuber, H. J. Is the Indian summer monsoon stable against global change? *Geophys. Res. Lett.* **32,** L15707 (2005).
83. Naidu, C. V. *et al.* Is summer monsoon rainfall decreasing over India in the global warming era? *J. Geophys. Res.* **114,** D24108 (2009).
84. Cobb, K. M. *et al.* Highly variable El Niño-Southern Oscillation throughout the Holocene. *Science* **339,** 67–70 (2013).
85. Zhang, Y., Wallace, J. M. & Battisti, D. S. ENSO-like interdecadal variability, 1900–93. *J. Clim.* **10,** 1004–1020 (1997).
86. Kumar, K. K., Rajagopalan, B. & Cane, M. A. On the weakening relationship between the Indian Monsoon and ENSO. *Science* **284,** 2156–2159 (1999).
87. Ashok, K., Chan, W.-L., Motoi, T. & Yamagata, T. Decadal variability of the Indian Ocean dipole. *Geophys. Res. Lett.* **31,** L24207 (2004).
88. Du. Y., Cai, W. & Wu, Y. L. A new type of the Indian Ocean Dipole since the mid-1970s. *J. Clim.* **26,** 959–972 (2013).
89. Annamalai, H., Hamilton, K. & Sperber, K. R. The South Asian summer monsoon and its relationship with ENSO in the IPCC AR4 simulations. *J. Clim.* **20,** 1071–1092 (2007).
90. Zhang, H. Diagnosing Australia-Asian monsoon onset/retreat using large-scale wind and moisture indices. *Clim. Dyn.* **35,** 601–618 (2010).
91. Zhang, H., Liang, P., Moise, A. & Hanson, L. The response of summer monsoon onset/retreat in Sumatra–Java and tropical Australia region to global warming in CMIP3 models. *Clim. Dyn.* **40,** 377–399 (2013).
92. Knutson, T. R. & Manabe, S. & Gu, D. Simulated ENSO in a global coupled ocean–atmosphere model: Multidecadal amplitude modulation and CO_2 sensitivity. *J. Clim.* **10,** 138–161 (1997).
93. Johnson, N. C. & Xie, S-P. Changes in the sea surface temperature threshold for tropical convection. *Nature Geosci.* **3,** 842–845 (2010).
94. Bony, S. & Dufresne, J. L. Marine boundary layer clouds at the heart of tropical cloud feedback uncertainties in climate models. *Geophys. Res. Lett.* **32,** L20806 (2005).
95. Schott, F. A., Xie, S. -P. & McCreary, J. P. Indian Ocean circulation and climate variability. *Rev. Geophys.*, **47,** RG1002 (2009).
96. Sprintall, J. & Tomczak, M. Evidence of the barrier layer in the surface layer of the tropics. *J. Geophys. Res.* **97,** 7305–7316 (1992).
97. Godfrey, J. S. & Lindstrom, E. J. The heat budget of the equatorial western Pacific surface mixed layer. *J. Geophys. Res.* **94,** 8007–8017 (1989).
98. Qu, T. & Meyers, G. Seasonal variation of barrier layer in the southeastern tropical Indian Ocean. *J. Geophys. Res.* **110,** C11003 (2005).
99. Masson, S., Boulanger, J-P., Menkes, C., Delecluse, P. & Yamagata, T. Impact of salinity on the 1997 Indian Ocean dipole event in a numerical experiment. *J. Geophys. Res.* **109,** C02002 (2004).
100. Qiu, Y., Cai, W., Li, L. & Guo, X. Argo profiles variability of barrier layer in the tropical Indian Ocean and its relationship with the Indian Ocean Dipole. *Geophys. Res. Lett.* **39,** L08605 (2012).

Additional information

Reprints and permissions information is available at www.nature.com/reprints. Correspondence and requests for materials should be addressed to W.C.

Acknowledgements

This work was supported by the Australian Climate Change Science Program, the National Basic Research Program of China (2012CB955600), the Goyder Research Institute, and the NFSC (41106010). M.C. was supported by the NERC SAPRISE project (NE/I022841/1). W.Y. was supported by the Chinese State Oceanic Administration Indian Ocean Climate Program.

Competing financial interests

The authors declare no competing financial interests.